REPORT DOCUMENTATION PAGE

Form Approved
OMB No. 0704-0188

1. REPORT DATE *(DD-MM-YYYY)*
10-08-2016

2. REPORT TYPE
FINAL

3. DATES COVERED *(From - To)*
01-June-14 to 30-June-16

4. TITLE AND SUBTITLE
Towards the use of HYCOM in Coupled ENSO Prediction: Assessment of ENSO skill in Forced Global HYCOM

5a. CONTRACT NUMBER

5b. GRANT NUMBER
N00014-14-1-0621

5c. PROGRAM ELEMENT NUMBER

6. AUTHOR(S)
Dr. Julie McClean and Dr. Bruce Cornuelle

5d. PROJECT NUMBER

5e. TASK NUMBER

5f. WORK UNIT NUMBER

7. PERFORMING ORGANIZATION NAME(S) AND ADDRESS(ES)
UNIVERSITY OF CALIFORNIA, SAN DIEGO
SCRIPPS INSTITUTION OF OCEANOGRAPHY
9500 GILMAN DRIVE
LA JOLLA, CA 92093-0210

8. PERFORMING ORGANIZATION REPORT NUMBER

9. SPONSORING/MONITORING AGENCY NAME(S) AND ADDRESS(ES)
Office of Naval Research
875 North Randolph Street
Arlington, VA 22203-1995

10. SPONSOR/MONITOR'S ACRONYM(S)

11. SPONSOR/MONITOR'S REPORT NUMBER(S)

12. DISTRIBUTION/AVAILABILITY STATEMENT
Public

13. SUPPLEMENTARY NOTES

14. ABSTRACT
A suite of ocean metrics was carried out to determine the veracity of the mean and variability of a global 0.08° configuration of the Hybrid Coordinate Ocean Model (HYCOM) in the tropical Pacific for 2003-2012. The mean east-west gradient of SSH along the equator was under-represented in the 0.08° HYCOM and upper-water column temperature biases were found with the water being too cold in the western basin and too warm in the eastern basin. It was hypothesized that the zonal Navy Operational Global Atmospheric Prediction System (NOGAPS) wind product used to force the model may be too weak in the tropics, especially in the far eastern Pacific. The HYCOM temperature time series at 100 m at the locations of the TAO/TRITON buoys spaced roughly 10-15° along the equator showed significant skill, except in the very far eastern region. HYCOM mixed layer depths were systematically shallower than the observations between 180°E and 140°W in the tropical Pacific throughout the year. To examine interannual variability and a greater number of ENSO events than were captured in the 10-year simulation, we used a global 0.72°

15. SUBJECT TERMS
ENSO, HYCOM, ocean modeling, skill assessment. metrics

16. SECURITY CLASSIFICATION OF:			17. LIMITATION OF ABSTRACT	18. NUMBER OF PAGES	19a. NAME OF RESPONSIBLE PERSON
a. REPORT	b. ABSTRACT	c. THIS PAGE			19b. TELEPHONE NUMBER *(Include area code)*

Towards the Use of HYCOM in Coupled ENSO Prediction: Assessment of ENSO Skill in Forced Global HYCOM

Julie L. McClean
Climate, Atmospheric Sciences, and Physical Oceanography Division
Scripps Institution of Oceanography
University of California San Diego
Mail Code 0230
La Jolla, CA 92093-0230
Phone: (858) 534-3030 Fax: (858) 534-9820 Email: jmcclean@ucsd.edu

Bruce Cornuelle
Climate, Atmospheric Sciences, and Physical Oceanography Division
Scripps Institution of Oceanography
University of California San Diego
9500 Gilman Drive, 0230
La Jolla CA 92093-0230
Phone: (858) 534 4021 Fax: (858) 534 9820 Email: bdc@uscsd.edu

Award Number: N00014-14-1-0621

LONG-TERM GOALS

Coupled ocean/atmosphere variability in the tropical Pacific, especially the El Niño/Southern Oscillation (ENSO), is a major contributor to fluctuations in North American and global rainfall and temperature, including tropical cyclones, extreme rainfall events, and droughts. Prediction of ENSO, even for the few months between the occurrence of westerly wind events in the western Pacific and the equatorial warming that triggers the Bjerknes feedback has been a major challenge. The long-term goal of this project is to contribute to the development and testing of a global fully coupled prediction system for the operational US Navy. The target time scales of this system will be seasonal through interannual; an essential capability of this system will be to forecast ENSO conditions with a reasonable degree of certainty.

OBJECTIVES

The project objective is to assess the skill of global Hybrid Coordinate Ocean Model (HYCOM) in the tropical Pacific. We evaluate the mean and variability of the region, particularly focusing on ENSO events. We investigated HYCOM forced with atmospheric fluxes from prediction systems and reanalysis, since both ocean and atmospheric components must first show skill in the uncoupled mode for coupled prediction to be successful. The simulations are not constrained by observations as we wish to make a base line assessment of HYCOM's skill based on the model's dynamics.

APPROACH

Global 0.08° HYCOM will be the ocean component of the Navy's future coupled prediction system, so its performance is of primary interest. At the inception of this grant, two simulations were available for analysis:

1. Global 0.08° HYCOM/CICE forced with Navy Operational Global Atmospheric Prediction System (NOGAPS) for 2003-2012. CICE is the Los Alamos National Laboratory sea ice model. The NOGAPS simulation was initialized from a 10-year HYCOM/CICE spun-up state forced with climatological surface atmospheric fluxes. This run was initialized from Generalized Digital Environmental Model 4 (GDEM4) climatological temperature and salinity. It was configured with 41 layers.
2. Global 0.72° HYCOM/CICE forced with NOGAPS for 2003-2012. The same initialization procedure as in (1) was used here but with a low-resolution spun-up state. It was also configured with 41 layers.

By comparing each of these simulations with observations, we can assess the individual skill of each simulation as well as any improvements in the representation of the tropical Pacific mean state when the simulation is mesoscale-eddy resolving rather than marginally eddy-permitting (telescopes to 0.5° at the equator). Consistent NOGAPS forcing was not available before 2003, so due to the limited length of these simulations we could not investigate interannual variability, rather we could only consider particular ENSO events. To understand how well HYCOM depicts the diversity of ENSO events over an extended period, we used an emerging version of global 0.72° HYCOM/CICE that was forced with an alternate set of atmospheric reanalysis fluxes. It is:

3. Global 0.72° HYCOM/CICE forced with Coordinated Ocean-Ice Reference Experiment 2 (CORE-II) corrected interannually varying fluxes (CIAF) for 1948-2009 (Large and Yeager, 2009). CORE-II reanalysis fluxes consist of National Center for Environmental Prediction (NCEP)/National Center for Atmospheric Research (NCAR) near-surface vector winds, temperature, specific humidity and temperature, and on a variety of satellite based radiation, sea surface temperature, sea-ice concentration, and precipitation products. It was initialized from Levitus-PHC2 climatology. It was configured with 32 layers.

A. Wallcraft (NRLSSC) provided simulation (1). We carried out simulation (2) using HYCOM/CICE codes provided by A. Wallcraft (NRLSSC), while A. Bozec and E. Chassignet (both FSU) provided simulation (3). None of the simulations were constrained by observations in order to obtain a base line assessment of the HYCOM's ability to produce the mean and variability of the tropical Pacific prior to the addition of data.

The depiction of the mean state and variability of the tropical Pacific by NOGAPS 0.08° HYCOM/CICE was evaluated using:

1. NOAA Tropical Atmosphere Ocean (TAO)/Triangle Trans-Ocean Buoy Network (TRITON) mooring array data: the array consists of 70 moorings deployed since the early 1990s across the entire Pacific basin in 11 meridional sections that span the equatorial waveguide. Primarily potential temperature and salinity, together with meteorological measurements, are available.

2. Equatorial Pacific mean Conductivity-Temperature-Depth (CTD)/Acoustic Doppler Current Profiler (ADCP) sections by Johnson et al. (2002).
3. Archiving Validation and Interpretation of Satellite Data in Oceanography (AVISO) altimetry: gridded (1/4°x1/4°) "all satellites merged" absolute sea surface height (DT-MADT) data are available since 1994.
4. Argo climatology: gridded horizontal maps of temperature and salinity are available at 10 m intervals from the surface down to 170 m, 20 m intervals down to 440 m, 50 m intervals down to 1350 m, and finally 100 m intervals down to almost 2000 m. Data was first available in about 2000, but the Argo array is only considered viable after about 2004 (Roemmich and Gilson, 2009).

A subset of skill assessments were performed using NOGAPS 0.72° HYCOM/CICE. ENSO statistics were calculated for the 60-year 0.72° HYCOM and compared with those from concurrent observations, using, among other analysis techniques, the "Climate Variability Diagnostics Package (CVDP)" developed by the NCAR Climate Analysis Section.

WORK COMPLETED

- We carried out a thorough skill assessment of the mean and variability of the tropical Pacific region of global 0.08° HYCOM/CICE using AVISO altimetry, Argo, mean CTD/ADCP sections and TAO/TRITON observations.

- We ran and carried out selected skill assessments of the 10-year NOGAPS global 0.72° HYCOM/CICE in the tropical Pacific for comparisons with global 0.08° HYCOM/CICE.

- We calculated ENSO statistics from a 60-year CORE2-CIAF global 0.72° HYCOM/CICE simulation that were compared with observational counterparts for 1948-2007.

RESULTS

We began our skill assessment of HYCOM by comparing mean sea surface height (SSH) from each of the NOGAPS-forced HYCOM simulations (0.08° and 0.72°) with that from the AVISO DT-MADT gridded product for years 2003-2012 in the tropical Pacific. The AVISO SSH was first interpolated onto the HYCOM grid and the spatial means were removed from both the model and the observations. In Fig.1, we show the mean SSH from AVISO (upper), 0.08° HYCOM (middle), and the bias or misfit (AVISO-HYCOM; lower). In the equatorial region (~5°N-5°S), HYCOM SSH is lower in the western Pacific and higher in the eastern Pacific relative to AVISO, and hence the simulated mean zonal SSH gradient is weaker than observed. The east-west difference across the Pacific basin is underestimated by approximately 10 cm near the equator (Fig. 1). Similarly, the low-resolution 0.72° counterpart (Fig. 2) shows a weaker simulated SSH gradient relative to observations, however in this case the spatial extents of the low bias in the west and the high bias in the east are reduced and increased, respectively. This systematic difference indicates that aspects of the mean circulation are inconsistent with observations; this is hypothesized to result from the zonal NOGAPS wind product used to force the model, which might be too weak in the tropics.

The veracity of 0.08° HYCOM potential temperature and salinity in the upper water column was assessed by comparing them to the Argo mapped product and to temperature observations from the NOAA TAO/TRITON array. In Fig. 3, we show mean potential temperature from Argo for 2006-2012 minus that from HYCOM for the same period at ~100m and 200m, and in zonal sections over the upper 500 m of the water column at 8°N,0, and 8°S. Significant mean biases are seen with respect to the Argo product, especially in the 100 m-200 m depth zone for both potential temperature and salinity (not shown). At the equator, average temperatures are underestimated by up to 2 degrees in the western part of the basin and overestimated by up to 2 degrees in the eastern part. The simulated thermocline tilt is too low, which is likely another symptom of weak mean wind forcing. Mean salinity misfits range from -0.2 to 0.4 (not shown), with HYCOM water being too fresh in the western part of the basin and too salty in the eastern part. Note that the temperature and salinity biases do not compensate in such as way that the pycnocline tilt matches that of Argo.

A complete set of mean and RMS misfits were calculated between the temperatures from the TOA/TRITON array and 0.08° HYCOM at 1m, 100m, 300 m, and 500m for 2004-2012. Time series of potential temperature for 2004-2012 at 100 m on the equator at the location of 9 TAO/TRITON moorings are shown in Fig. 4 from 0.08° HYCOM, the mooring data, and Argo data. The variability of temperature and salinity (not shown) is captured quite well at the equator in the thermocline. The agreement with the TAO observations is similar to the agreement with the Argo mapped product. While there are mean biases, the variability is represented relatively well for the moorings west of 95°W, where the fraction of TAO variance captured by HYCOM ranges from 20% to 78% (the sparseness of observations and low variance at 95°W likely result in particularly poor skill). However, away from the equator model skill is poor in some parts of the tropical domain, with the ratio of misfit variance to observed variance exceeding 1 (meaning that the simulation has no skill in reproducing observations) over large regions of the domain (not shown).

Climatological 0.08° HYCOM temperature, salinity and zonal velocity were compared with the cross-equatorial CTD/ADCP sections of Johnston et al. (2002). Finally, monthly climatological mixed layer depths (MLDs) obtained from Argo profiles (Holte et al. 2016) and 0.08° HYCOM were compared using a threshold density crierion. HYCOM MLDs were systematically shallower than the observations between the 180°E and 140°W in the tropical Pacific throughout the year.

Although the 10-year model integration is too short to resolve interannual variability, it is possible to use Hovmöller diagrams to qualitatively track ENSO cycles along the equator. Time-longitude diagrams of SSH anomalies (m) in the equatorial Pacific in 0.08° HYCOM and AVISO are found in Fig. 5. Anomalies are defined as the departure from the mean SSH (Fig. 1) and are averaged between 1°S and 1°N. The plots clearly show the ENSO cycle, which is generally well captured by HYCOM. As well, we can examine ENSO indices during this period to see if the magnitude and phasing of the ENSO events are in accordance with observations, as well as the diversity of events. In Fig. 6, the geographic regions representing the Niño 1.2, 3, 3.4, and 4 indices are overlaid on observed sea surface temperature (SST; Reynolds and Smith, 1994) for January 1983. Niño indices for 2003-2012 from NCEP observations (upper), 0.08° HYCOM/CICE (middle), and 0.72° HYCOM/CICE (lower) are seen in Fig. 7. In the central Pacific (Niño 4, 3.4, and 3) anomalies are strongest during 2009/10, while in the eastern Pacific (Niño 1.2) anomalies are strongest during 2011 and 2012 events. HYCOM anomalies from both simulations track with the observations for the 2009/10 and 2011 events, but in 2012 the HYCOM anomalies are weaker than those observed. Correlations of the Niño 1.2, 3, 3.4, and 4 SST indices from 0.08° HYCOM/CICE and observations are 0.67, 0.72, 0.67, and 0.97, respectively, whereas those from data and 0.72° HYCOM/CICE are 0.65,0.7, 0.67, and 0.89. In both cases, the eastern index is the poorest performer.

To further examine the representation of ENSO events in HYCOM, we now consider results from the 60-year 0.72° HYCOM run forced with CORE-II CIAF. Seasonal and annual means and variability of global sea surface temperature (SST), time series and spectra of Niño climate indices, and ENSO spatial composites were calculated for this HYCOM run and concurrent Hadley Centre Sea Ice and SST (HadISST) observations (Rayner et al., 2003). We used CVDP (Phillips et al. 2014) to carry out these calculations. We also calculated empirical orthogonal functions of SST from HadISST and this model run. Following the model spin-up period (first 2 decades of the run), the time series of HYCOM Niño 1.2, 3, 3.4, and 4 SST indices all showed reasonable agreement with those based on observations, with HYCOM Niño 3.4 and 4 showing the best agreement and Niño 1.2 the least good agreement (not shown). The power spectrum of the Niño 3.4 SST index is shown in Fig. 8 for detrended HadISST (upper) and HYCOM SST (lower) for 1948-2007. The model reproduces the double-peak structure spanning years 3.5-8, with the maximum peak at ~5-5.5 years being 1.2 times stronger in the model than in the observations.

Longitude-time plots of composite SST anomalies along the equator (3°N-3°S) for the warm (El Niño) and cold (La Niña) phases of ENSO from the HadISST observations and global 0.72° HYCOM/CICE for 1948-2007 are shown in Fig. 9. ENSO composites were obtained from the normalized December Niño3.4 timeseries; all years greater than 1 standard deviation and all years less than -1 standard deviation were composited to represent El Niño and La Niña conditions, respectively. The spatial structure and timing of the simulated SST anomalies for both ENSO phases are in good agreement with that from observations.

CONCLUSIONS

The goal of this project was to assess the skill of global HYCOM in the tropical Pacific, particularly the ability of the model to realistically represent ENSO. Since 0.08° HYCOM will be the ocean component of the Navy's future coupled prediction system, its performance was of primary interest. A suite of ocean metrics was carried out to determine the veracity of its mean state and variability. The mean east-west gradient of SSH along the equator was under-represented in the 0.08° HYCOM and upper-water column temperature biases were found with the water being too cold in the western basin and too warm in the eastern basin. It is hypothesized that the zonal NOGAPS wind product used to force the model may be too weak in the tropics, especially in the far eastern Pacific. The HYCOM temperature time series at 100 m at the locations of the TAO/TRITON buoys spaced roughly 10-15° along the equator showed significant skill, except in the very far eastern region. Away from the equator in the tropical region there were also patches where the ratio of misfit variance to observed variance indicated that the model simulation had no skill. HYCOM mixed layer depths were systematically shallower than the observations between 180°E and 140°W in the tropical Pacific throughout the year. The 10-year 0.08° HYCOM simulation was of insufficient length to be able to assess interannual variability, however time-longitude (Hovmöller) diagrams of SSHA along the equator clearly showed ENSO cycles to be well represented by the model. As well, Niño SST indices from 0.08° HYCOM/CICE and observations were well correlated, with the most western Pacific Niño index having the highest skill and the eastern Pacific index having the lowest.

To examine interannual variability and a greater number of ENSO events, we used a recent global 0.72° HYCOM/CICE simulation that was forced with CORE-II CIAF for 1948-2007. Due to differences in the NOGAPS and CORE- forced simulations set-up such as the spin-up and the length of the simulations we do not report direct comparisons between this run and the NOGAPS runs. The

CORE-forced simulation realistically represented both the Niño SST indices, the spectral characteristics of the Niño 3.4 SST index, and the structures and number of occurrences of El Niño and La Niña events during 1948-2007. Consequently, it is expected that emerging 0.08° HYCOM/CICE simulations forced with CORE-II CIAF will provide realistic yard-sticks for comparisons with future simulations where 0.08° HYCOM is the ocean component of fully coupled models.

IMPACT/APPLICATIONS

Improved realism of ENSO events in the Navy's operational coupled ocean/sea-ice prediction system should reduce uncertainty in predictions and provide increased confidence in projections for decision making.

RELATED PROJECTS

"Optimized Infrastructure for the Earth System Prediction Capability"; Celicia DeLuca (PI). A goal of this project is to incorporate HYCOM into CESM.

REFERENCES

Deser, C., A. S. Phillips, R. A. Tomas, Y. Okumura, M. A. Alexander, A. Capotondi, J. D. Scott, Y. -O. Kwon, and M. Ohba, 2012: ENSO and Pacific Decadal Variability in Community Climate System Model Version 4. *J. Climate*, 25, 2622-2651.

Holte, J., J. Gilson, L. Talley and D. Roemmich, 2016: Argo Mixed Layers, Scripps Institution of Oceanography/UCSD http://mixedlayer.ucsd.edu, (accessed [2014]).

Large, W. G., and S. G. Yeager, 2009: The global climatology of an interannually varying air-sea flux data set. *Clim. Dyn.*, 33, 341-364.

Phillips, A.S., C. Deser, and J. Fasullo, 2014: A new tool for evaluating modes of variability in climate models, EOS, 95, 453-455, doi: 10.1002/2014EO490002.

Rayner, N. A., D. E. Parker, E. B. Horton, C. K. Folland, L. V. Alexander, and D. P. Rowell, E.C. Kent, and A. Kaplan, 2003: Global analyses of sea surface temperature, sea ice, and night marine air temperature since the late nineteenth century, *J. Geophys. Res.*, 108, No. D14, 4407, doi:10.1029/2002JD002670.

Roemmich, D. and J. Gilson, 2009: The 2004-2008 mean and annual cycle of temperature, salinity, and steric height in the global ocean from the Argo Program. *Progr. Oceanogr.,* 82, 81-100.

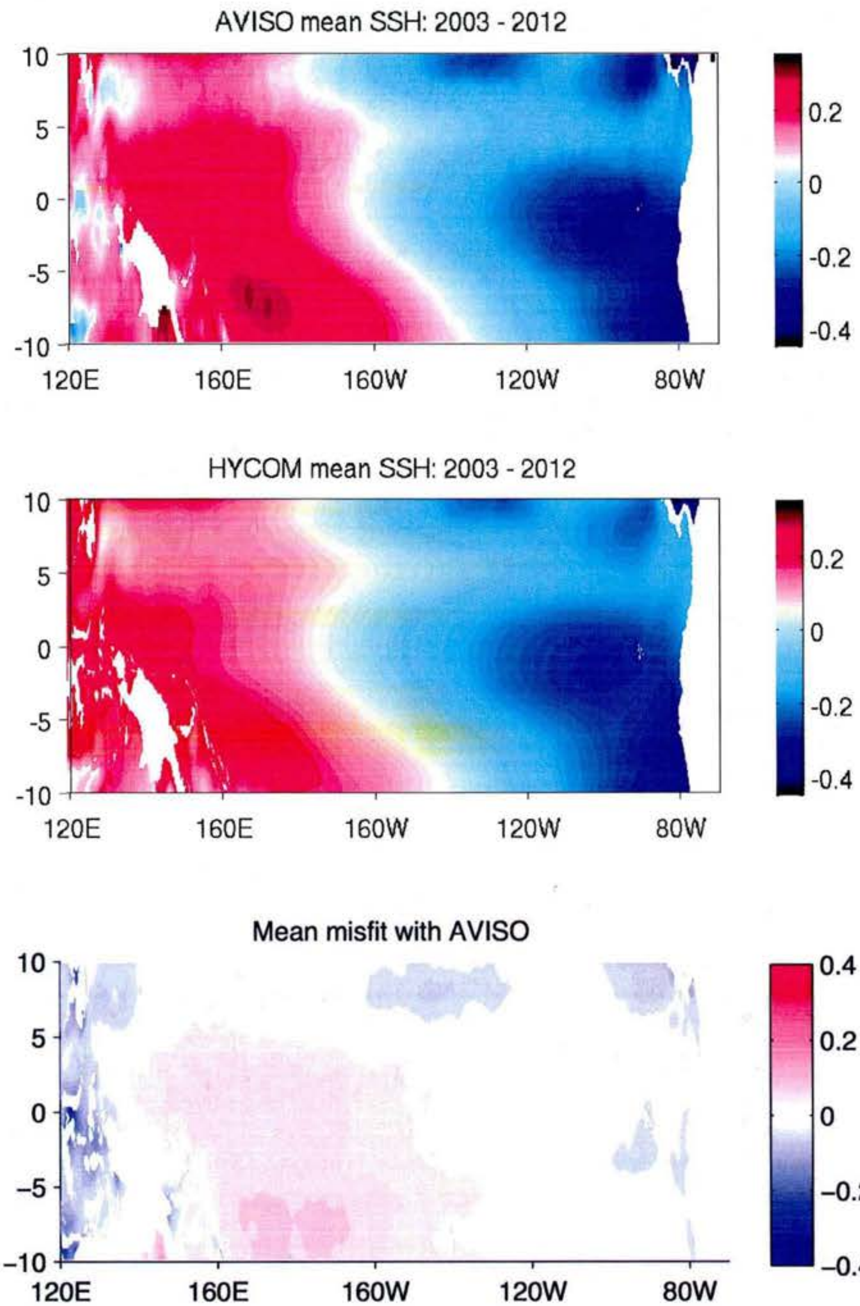

Fig. 1: The 2003-2012 mean SSH (m) in 0.08° global HYCOM (a) is compared to the gridded AVISO product for the same period (b). The spatial mean is removed from both datasets. The difference "AVISO minus HYCOM" (c) highlights discrepancies in the mean circulation, perhaps due to the strength of the wind stress product used to force HYCOM.

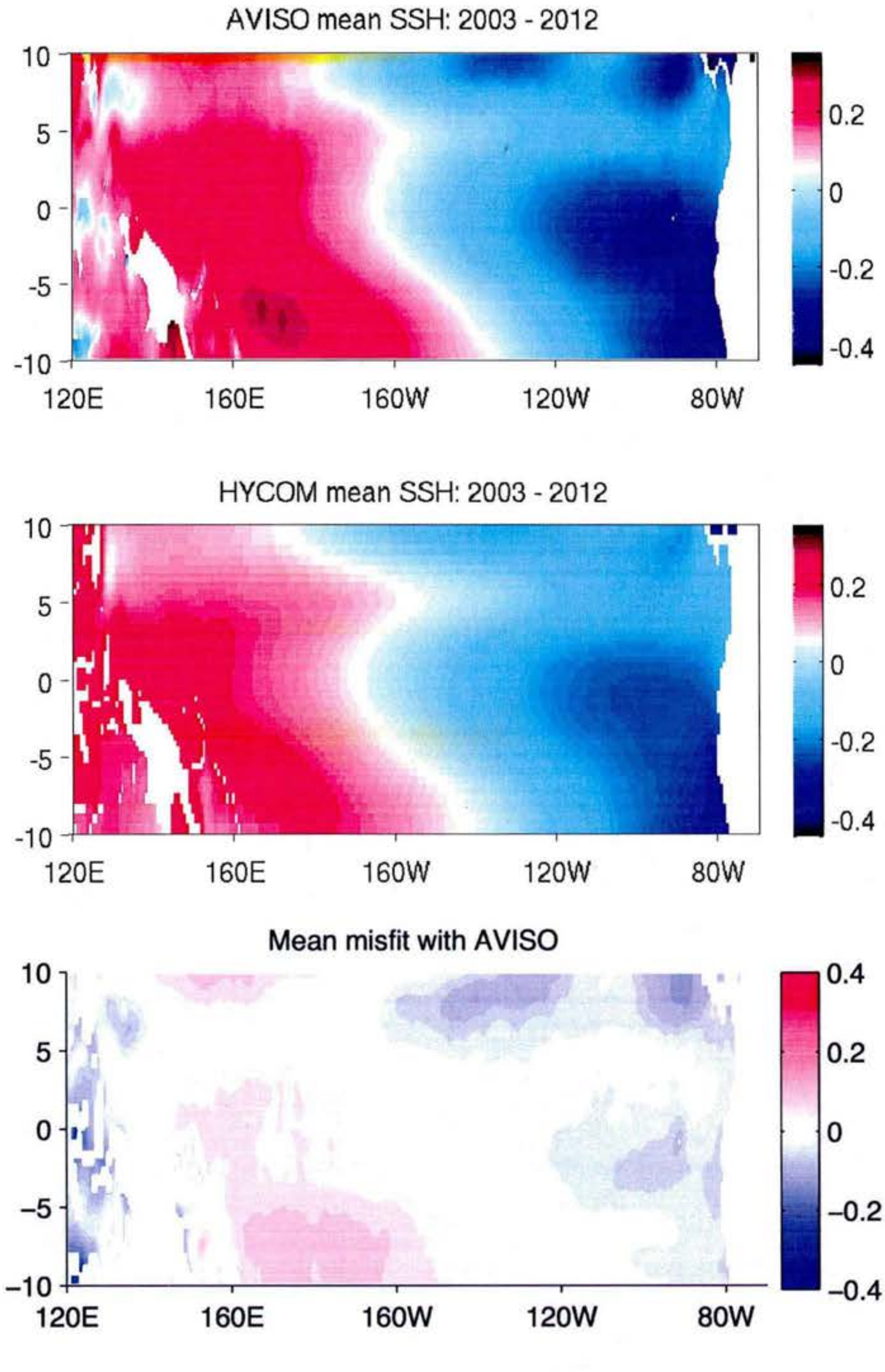

Fig. 2: The 2003-2012 mean SSH (m) in 0.72° global HYCOM (NOGAPS forcing) (a) is compared to the gridded AVISO product for the same period (b). The spatial mean is removed from both datasets. The difference "AVISO minus HYCOM" (c) highlights discrepancies in the mean circulation, perhaps due to the strength of the wind stress product used to force HYCOM.

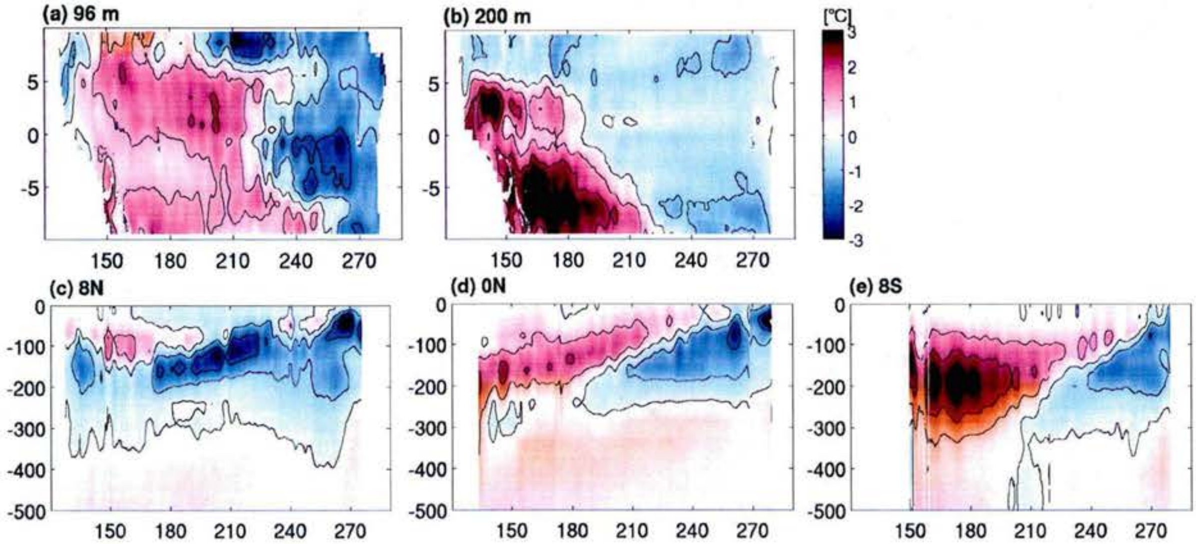

Fig. 3: Potential temperature bias of 0.08° HYCOM using the Argo mapped product for the tropical Pacific basin. Mean of "Argo minus HYCOM" for 2006-2012 at (a) 96 m, (b) 200 m, and (c) zonal sections at 8°N, (d) 0°N and (e) 8°S. The mean misfit shows significant biases, especially in the 100 m-200 m depth range

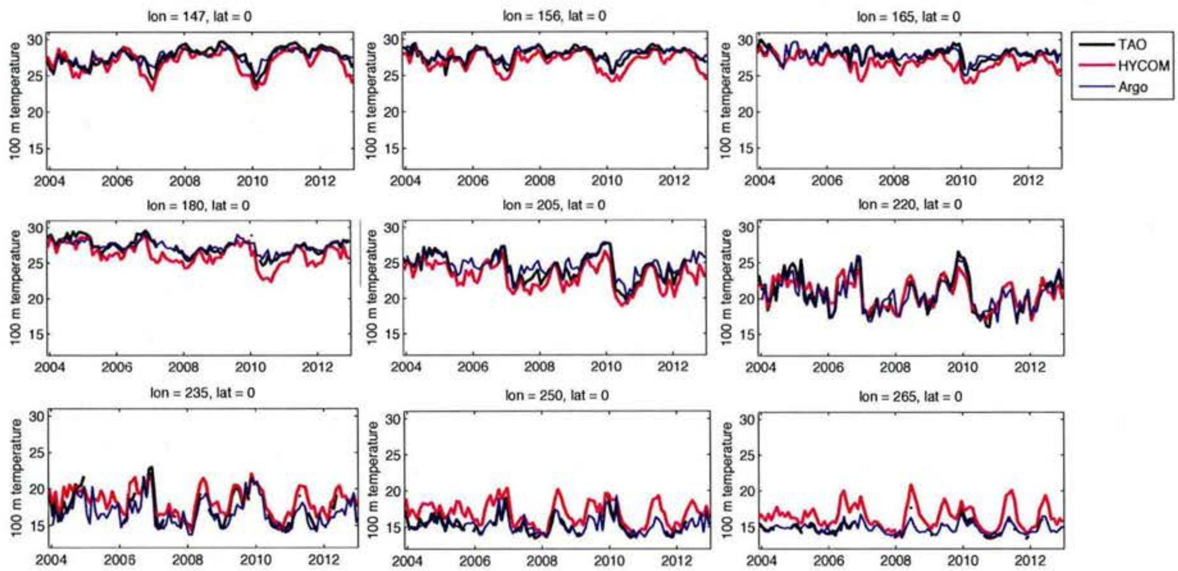

Fig. 4: Time series of potential temperature (°C) for 2004-2012 at 100 m along the equator at 147°E, 156°E, 165°E, 180°E, 155°E, 140°E, 125°W, 110°W, and 95°W from the TAO moorings (black), 0.08° HYCOM (red) and the Argo mapped product (blue). Observed variability is reproduced relatively well by HYCOM.

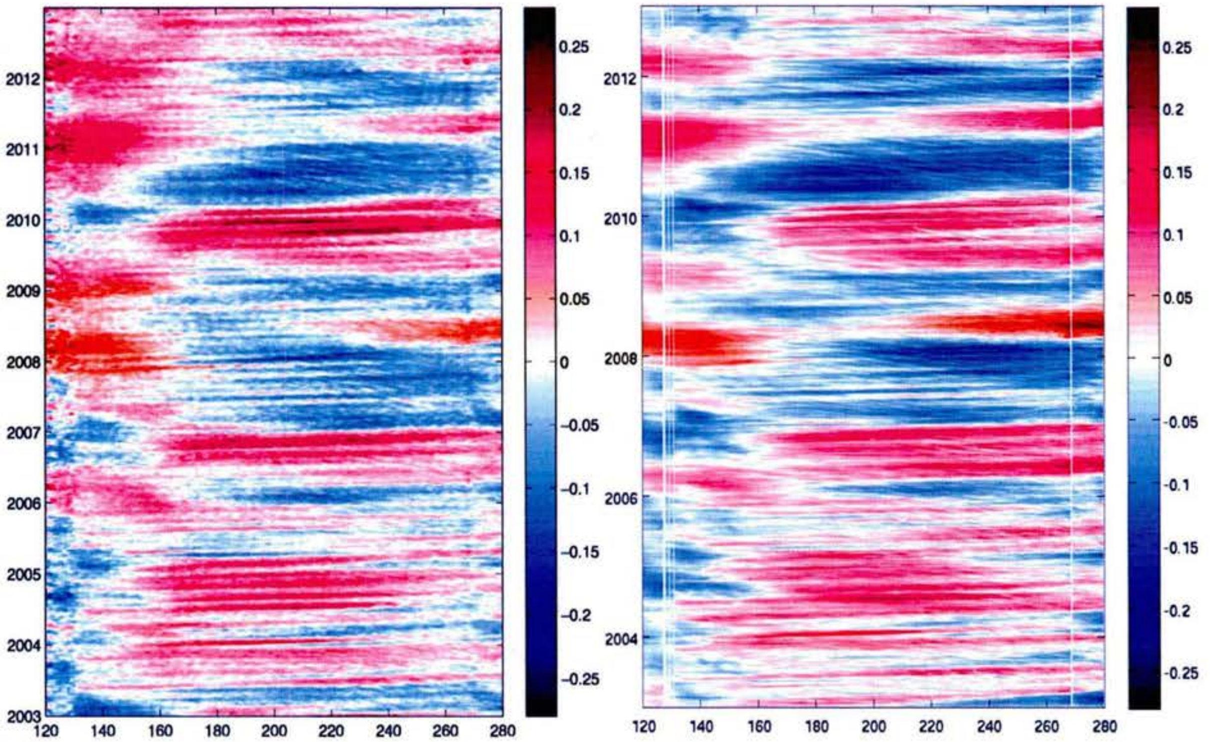

Fig. 5: Time-longitude diagram of SSH anomalies (m) in the equatorial Pacific from AVISO (left) and 0.08° HYCOM/CICE (right). Anomalies are defined as the departure from the mean SSH (Figure 1) and are averaged between 1°S and 1°N. The plots clearly show the ENSO cycle, which is generally well captured by the model.

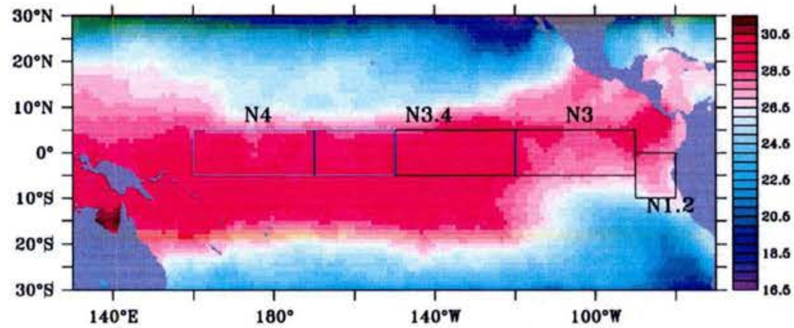

Fig. 6: Observed SST (Reynolds and Smith, 1994) for January 1983 overlaid with geographic regions representing the Niño 1.2, 3, 3.4, and 4 indices. Black thick line = Nino1.2 (0 - 10°S, 80°W-90°W); Black thin line = Nino 3 (5°N-5°S, 90°W - 150°W); Blue thick line = Nino3.4 (5°N-5°S 120°W - 170°W); Green thin line = Nino 4 (5°N -5°S, 160°E - 150°W).

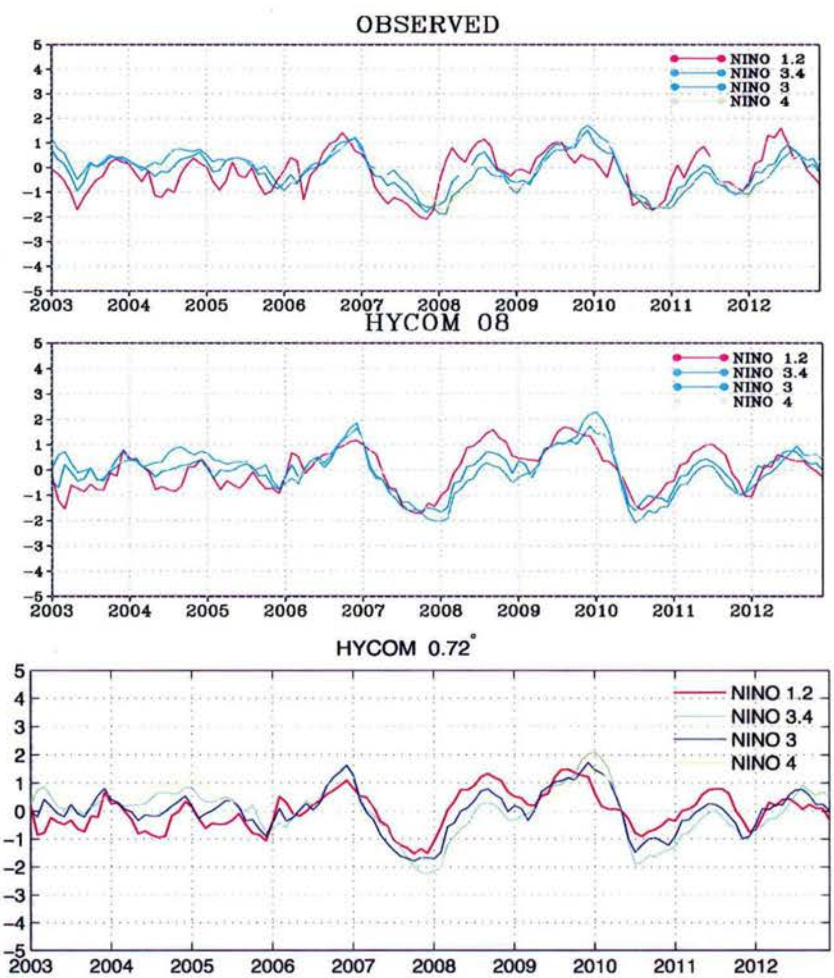

Fig. 7: Time series of Niño indices for 2003-2012. Indices from NCEP: *ftp://ftp.cpc.ncep.noaa.gov/wd52dg/data/sstoi.indices* (upper), 0.08° HYCOM/CICE (middle), and 0.72° HYCOM/CICE (lower). Both simulations are forced with NOGAPS

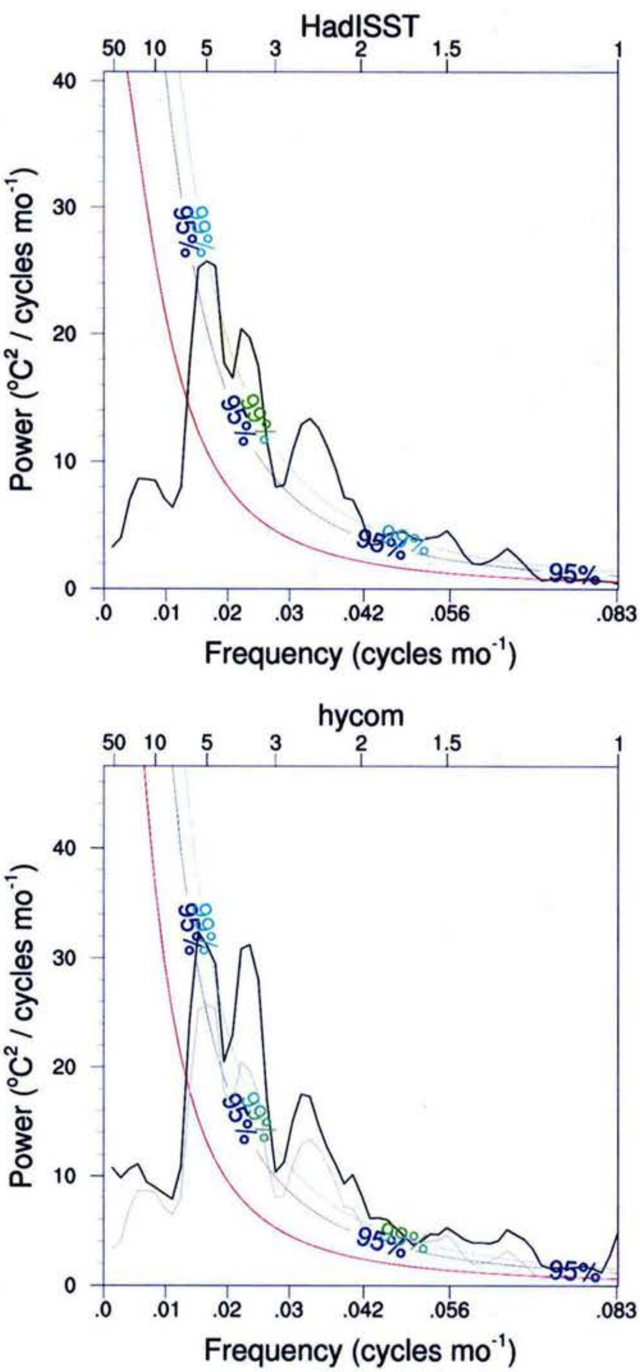

Fig. 8: Power spectrum of the Niño 3.4 SST index for 1948-2007 using detrended HadISST (upper) and 0.72° HYCOM/CICE SST forced with CORE-II CIAF (lower). Figure produced using NCAR's CVDP package.

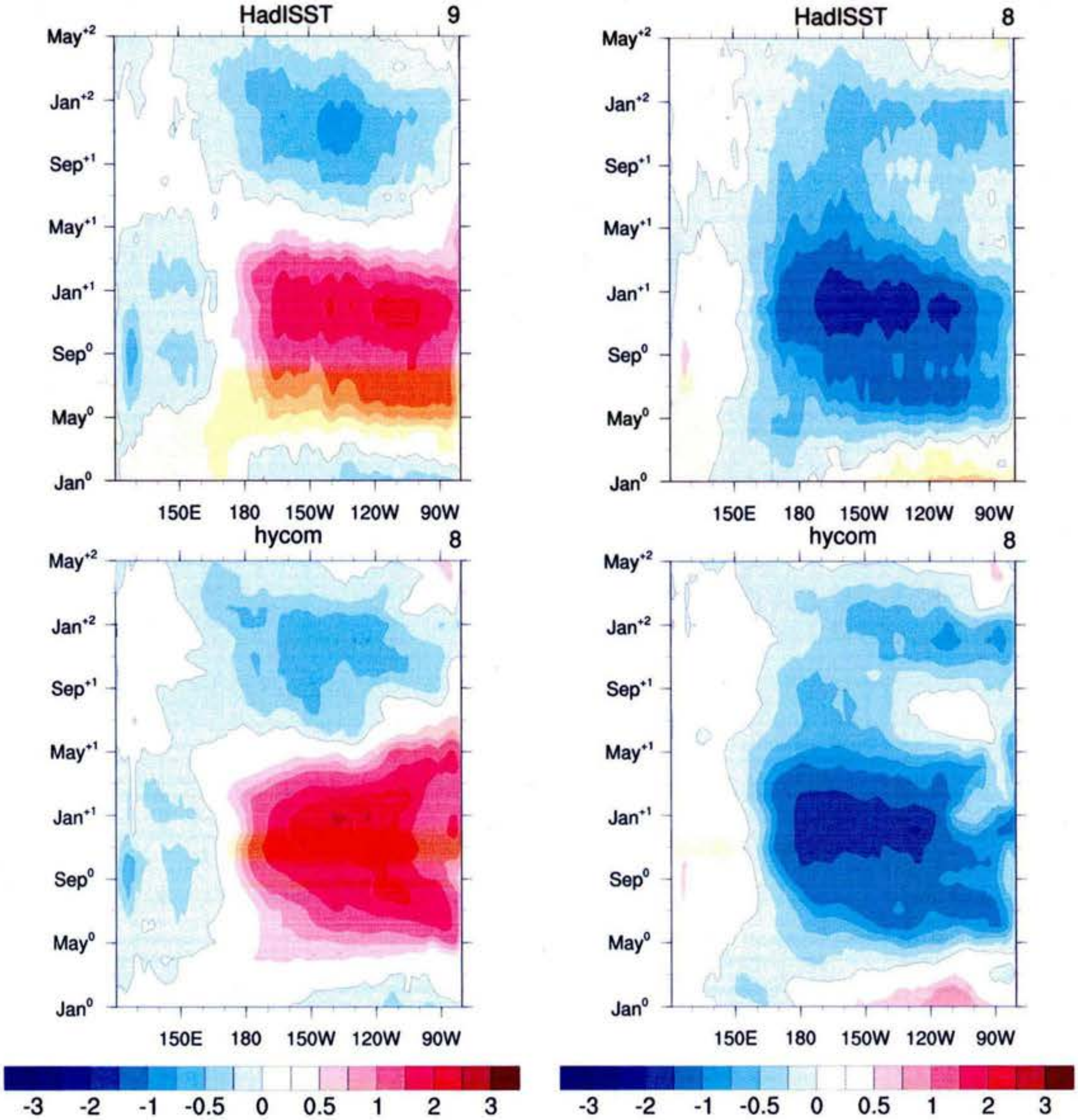

Fig. 9: Longitude-time plots of composite SST anomalies along the equator (3°N-3°S) for El Niño (left) and La Niña (right) based on HadISST observations (upper) and global 0.72° HYCOM/CICE forced with CORE-II CIAF (lower) for 1948-2007. The number in the upper right hand corner above each plot indicates the number of events used in the composite. Figure produced using NCAR's CVDP package.